한국해양공학회지 제19권 제6호, pp 1~7, 2005 (ISSN 1225-0767)

Aerodynamic Characteristics of Impulse Turbine with an End Plate for Wave Energy Conversion

BEOM-SOO HYUN*, JAE-SEUNG MOON*, SEOK-WON HONG** AND KI-SUP KIM**
*Division of Ocean Systems Engineering, Korea Maritime University, Busan, Korea
**Korea Research Institute of Ships and Ocean Engineering, Daejeon, Korea

KEY WORDS: Wave Energy, Impulse Turbine, End Plate, CFD, Tip Penetration, Vortex Roll-up, Cooper Mesh, Tip Clearance

ABSTRACT: *This paper deals with the design and aerodynamic analysis of a special-type impulse turbine, with an end plate for wave energy conversion. Numerical analysis was performed using a CFD code, FLUENT. The main idea of the proposed end plate was to minimize the adverse effect of tip clearance of turbine blade, and was borrowed from ducted propeller, with so-called penetrating end plate for special purpose marine vehicles. Results show that efficiency increases up to 5%, depending on the flow coefficient; a higher flow coefficient yields increased efficiency. Decrease of input coefficient CAwith an end plate is the main reason for higher efficiency. Performance of end plate at various design parameters, as well as flow conditions, was investigated; the advantages and disadvantages of the presentimpulse turbine were also discussed.*

1. Introduction

An impulse turbine has recently been recognized as one of the most effective wave energy conversion device because of its wide operating range of flow rates, low rotor speed and good self-starting characteristics. The present study has been conducted as a part of an on-going project on the development of a prototype OWC-Impulse turbine system commenced last year at Korea Research Institute of Ships and Ocean Engineering in Korea (Hong, 2004). Some of the numerical approaches on parametric study of impulse turbine were introduced in Hyun et al. (2004) in general and Hyun and Moon (2004) with more precise numerical treatment. These numerical approaches adopted Reynolds-averaged Navier-Stokes' (RANS) equations, while the LES calculation may provide information on different aspects especially for unsteady fully separating flow (Setoguchi et al., 2004).

This paper deals with the design of a special-type impulse turbine having an end plate for wave energy conversion. The main idea of the proposed end plate was to minimize the adverse effect of tip clearance of turbine blade, and borrowed from ring-type propeller housed in duct for special purpose marine vehicles. Two different configurations were considered in the present investigation as follows

(a) Simple penetration of blade into duct : It is well-known that minimizing the tip clearance improves the turbine efficiency. Since it is impossible to make the tip clearance zero, the idea of penetrating the blade tip in to duct is devised to make the tip clearance virtually zero. It is called the simple penetration of blade. However, it is found later in this paper that the simple penetration is not the effective means at all.

(b) Penetrating end plate : Second idea comes from the so-called "ring propeller" installed inside a shroud in marine propeller design, and similarly the winglet of jumbo airplane currently operated. It is properly designed end plate mounted vertically on the blade tip of rotor to minimize the interaction between the high and low pressure regions across the lifting surface through the wing tip and thus to reduce the induced drag. We call it here "End Plate".

Study was performed numerically using a code, FLUENT. Turbine geometry of Setoguchi et al., (2001) was selected as a basic turbine model. Full three-dimensional calculation was performed to find out optimum principal particulars. The performance of end plate at various design parameters as well as flow conditions was also investigated.

2. Turbine Geometry, Numerical Method and Test Conditions

Turbine geometry of Setoguchi et al., (2001) was selected as a basic turbine model, since it was known to be one of the best impulse turbine ever designed. Impulse turbine rotor with the diameter (D) of 38cm contains 30 rotor blades (z=30) and has a hub ratio of 0.7. Blade axial chord (l_r) and span (b) are 6.84cm and 5.7cm, respectively. Fig. 1 shows the turbine geometry and provides some brief dimensions. Tip clearance was 1mm, and more details can be found in Hyun et al.

제1저자 현범수 연락처: 부산광역시 영도구 동삼동 1번지
051-410-4308 bshyun@mail.hhu.ac.kr

(2004). Geometry of end plate is shown in Fig. 2. The end plate attached to the tip of the normal turbine blade is approximately 15% bigger in axial chord length l_r compared to original blade section, and the shape of blade section was managed to keep the same as much as possible. Thickness of end plate was chosen to be 0.5mm (0.13% of rotor diameter).

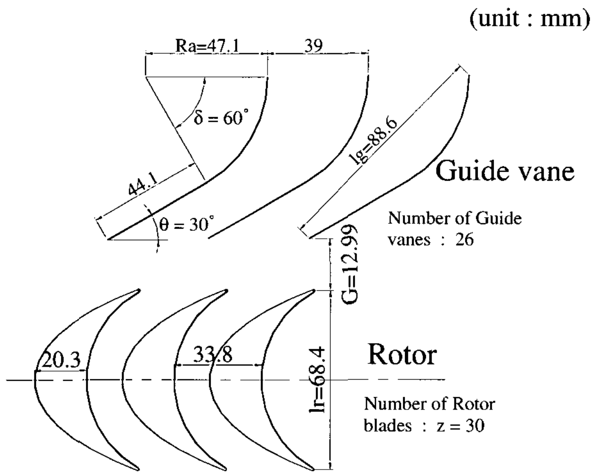

Fig. 1 Turbine Geometry

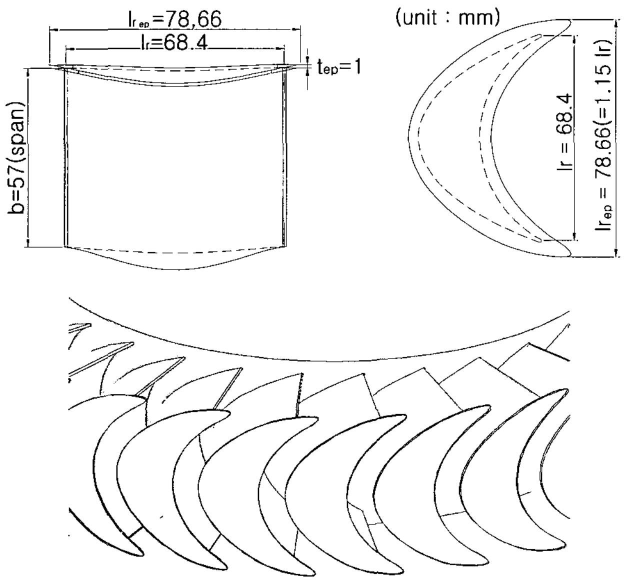

Fig. 2 Configurations of End Plate

A commercial CFD code, FLUENT 6.1.22, was employed in the present numerical analysis. Full three-dimensional calculation was performed to find out optimum principal particulars. A relative moving reference frame was adopted for the rotor blade. Axial flow was considered as a constant axial velocity for the numerical approach using steady analysis, since its frequency is considerably low compared to the harmonics of a rotational blade-to-blade flow of turbine. The k-ε model was employed for turbulent flow (Hong, 2004). The GAMBIT 2.1.6 was used for grid generation. An unstructured grid system using a tetrahedral mesh was adopted. Since it is very important to capture the detailed flow structure in the narrow gap between rotor tip and duct where unstructured grid works poorly, multiple layers of Cooper-type mesh were introduced in gap region. The number of meshes was determined to be 500,000 by examining the grid dependency on numerical accuracy (Hyun and Moon, 2004).

The range of blade Reynolds number varied from $5\text{x}10^4$ ~ $3\text{x}10^5$, where the Reynolds number was defined based on blade chord and the resultant flow velocity (vector sum of inflow and rotation speed of rotor blade). Although the magnitude of axial velocity components were set to 15m/s a for standard case, those value was not strictly controlled for calculation, since the effect of Reynolds number in a range of present calculation was found to be relatively minor (Hyun and Moon, 2004). While flow was assumed to be either laminar or turbulent, the results showed only a slight difference regardless of flow condition (Hyun and Moon, 2004). Performance of the impulse turbine in the steady flow condition is expressed in terms of the input coefficient C_A and the torque coefficient C_T as follows;

$$C_A = \frac{\Delta p Q}{\frac{1}{2}\rho_a(v_a^2 + U_R^2)bl_r z v_a}$$

$$C_T = \frac{T}{\frac{1}{2}\rho_a(v_a^2 + U_R^2)bl_r z r_m} \tag{1}$$

Here Δp, Q, T represent pressure drop, flow rate and torque, and v_a, U_R, r_m are axial mean velocity, rotational velocity of rotor blade at $r = r_m$ and radius at mid-span, respectively. The efficiency of turbine η and the flow coefficient ϕ can be expressed as follows;

$$\eta = \frac{Tw}{\Delta p Q} = \frac{C_T}{C_A \phi}$$

$$\phi = v_a / U_R \tag{2}$$

where flow coefficient ϕ has a physically equivalent meaning with the angle of attack in wing theory.

3. Results and Discussions

3.1 Effect of End Plate

Before discussing the effect of end plate, the quality of present calculation was examined for the original turbine without an end plate, for which experimental data are available (Setoguchi et al., 2001). Fig. 3 shows the comparisons between experiment and calculations for G/l_r=0.19, where G denotes the gap between guide vane and rotor. In fact, the calculation with 4 layers of cooper-type mesh in tip region was made for more careful treatment of tip region compared to standard unstructured grid adopted in previous paper (Hyun et al., 2004). Result shows that calculations with cooper-type mesh in tip region provide better agreements in efficiency with a little lower pressure drop (lower C_A) and torque coefficient C_T.

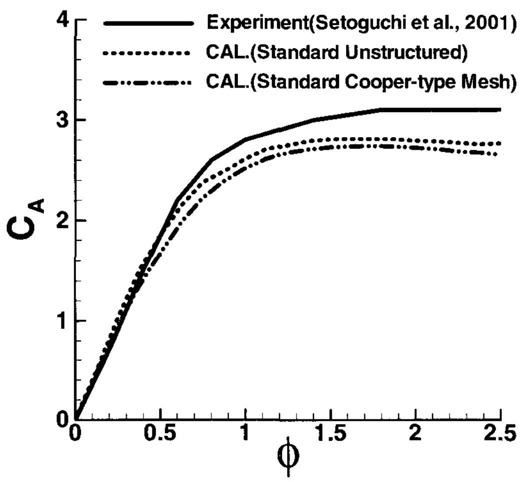

(a) Input Coefficients C_A

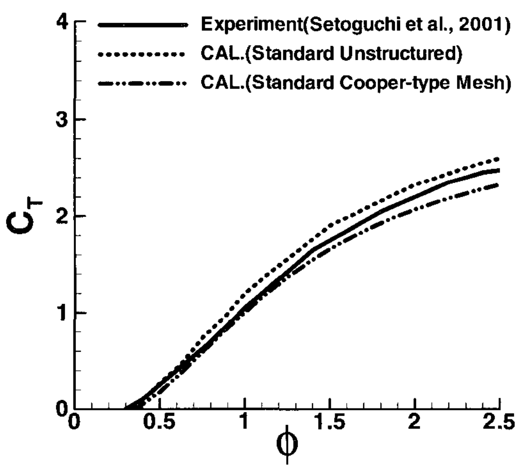

(b) Torque Coefficients C_T

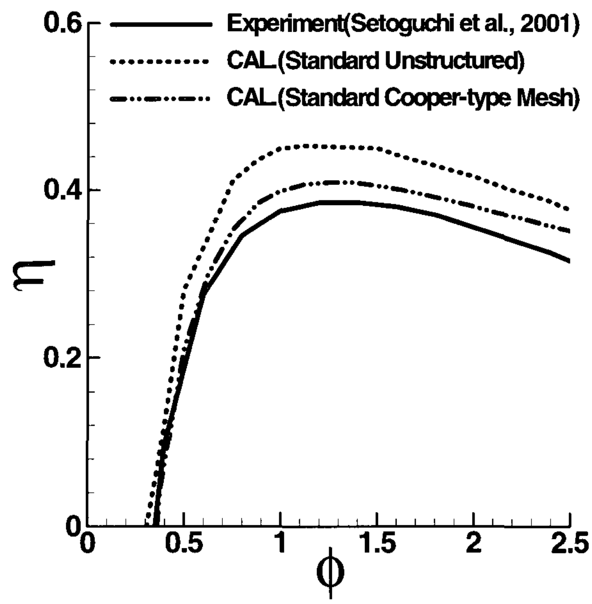

(c) Turbine Efficiency η

Fig. 3 Comparison Between Experiments and Calculations for Original Rotor

Fig. 4 demonstrates the effect of end plate, where all 3 calculations (original turbine, simple penetration, end plate) were compared together. The case of simple penetration turned out that it didn't improve the performance of turbine at all, although it was expected to minimize the adverse effect of tip clearance of turbine blade by alteration of flow passage. The efficiency was found to be almost independent of penetrating depth by further numerical investigation (not shown here for brevity), leading the conclusion that the simple penetration is not the effective means.

With an end plate, however, the efficiency increases with increasing flow coefficients. It is found that an end plate provides 3~5% improvements in efficiency with flow coefficient higher than ϕ=1. Decrease of input coefficient C_A with an end plate is the main reason of higher efficiency, while torque coefficient C_T is almost invariant. Fig. 5 shows the flow pathlines on suction and pressure sides of rotor blade at ϕ = 1 for all 3 cases. Flow direction is downward in this figure. Clear evidence of tip vortex roll-up is visible for first two cases around trailing edge region near tip (right bottom corner) of suction side. End plate was found to effectively prevent the flow interaction between suction side and pressure side, and consequently the vortex roll-up, yielding well-aligned flow field near tip region (parallel to mid-span flow) on suction side. Effect of end plate on pressure side was relatively minor compared to suction side.

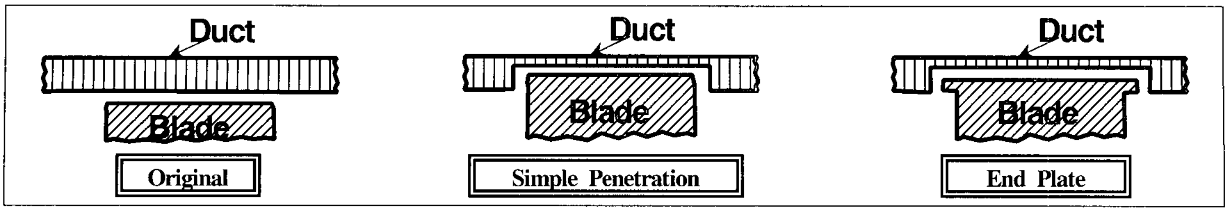

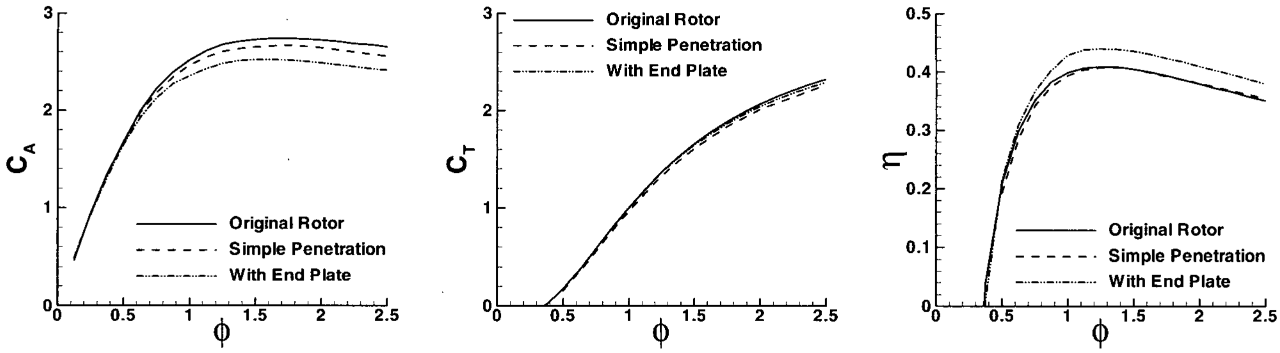

(a) Input Coefficients C_A (b) Torque Coefficients C_T (c) Turbine Efficiency η

Fig. 4 Effect of End Plate

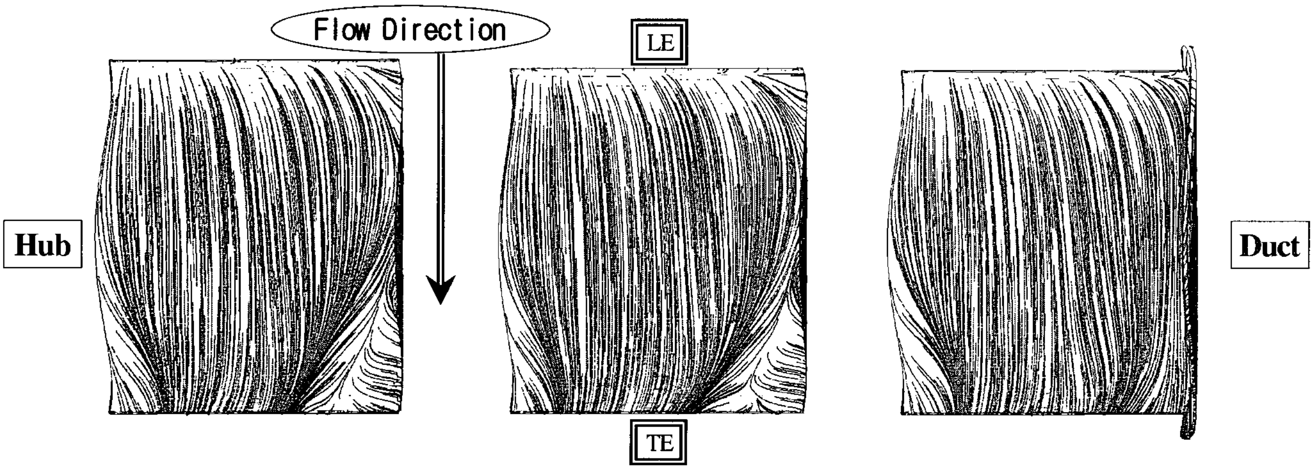

(a) Original Rotor (b) Simple Penetration (c) With End Plate

Fig. 5 Flow Pathlines on Suction Side of Rotor (ϕ=1)

3.2 Effect of Thickness of End Plate

Now we see the effect of thickness of end plate, tep. Four different thicknesses were chosen; 0.5mm, 1mm, 3mm, 5mm, which correspond to 0.13, 0.26, 0.79 and 1.32% of rotor diameter, respectively. These results are compared to that of original rotor without an end plate in Fig. 6. The thinnest end plate seems to produce best efficiency even though the effect of thickness is not significant. It is obviously the pressure dominant flow, since the variation of viscous drag by thickness effect of end plate was found to be negligible. Interestingly, the thinner end plate works better with lower flow coefficient (ϕ<1), while the thicker end plate better with higher flow coefficient (ϕ>2). The thickness variation is mainly changing the input coefficient, meaning the pressure loss in flow passage is affected by plate thickness more or less.

The streamline patterns on the upper surface of end plate at ϕ=1 were plotted in Fig. 7. Almost same streamline pattern with that of original rotor was obtained with t_{ep}=1mm (t_{ep}*= $t_{ep}/D\times100$ = 0.26). On the other hand, flow on the upper surface of end plate with t_{ep}=5mm (t_{ep}*=1.32) is parallel to the direction of rotor rotation without any chordwise flow, the indication of no axial flow passing through this gap between blade and duct. The reason of the thickness effect was however not clearly understood up to the present stage.

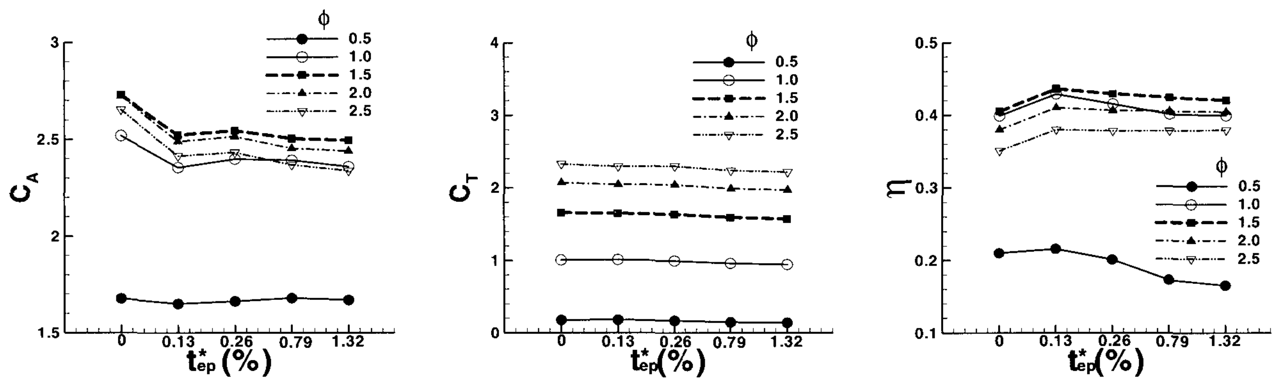

(a) Input Coefficients C_A (b) Torque Coefficients C_T (c) Turbine Efficiency η

Fig. 6 Effect of Thickness of End Plate

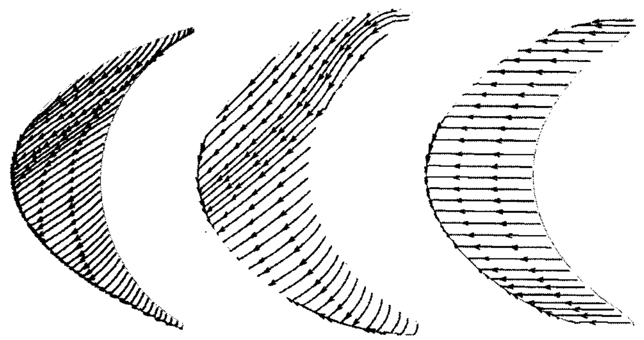

(a) Original Rotor (b) End Plate(t^*_{ep}=0.26%) (c) End Plate(t^*_{ep}=1.32%)

Fig. 7 Limiting Streamlines on Tip Surface of Rotor Blade

3.3 Effect of Chord Length of End Plate

Effect of chord length of end plate was investigated for $1.15<C_{ep}<1.3$, where C_{ep} denotes the ratio of axial chord length of end plate to that of original rotor, and C_{ep}=1.15 represents the originally designed value. Maximum value of C_{ep} was restricted to 1.3 by keeping z=30, while G/l_r had to be changed from 0.19 to 0.37 for this calculation to accomodate larger size end plate in rotor area. Performance curves with the variation of chord length are shown in Fig. 8, together with all 3 shapes of end plate. C_A tends to decrease with increasing axial chord length while C_T is almost invariant, consequently some improvements in efficiency being achieved for $\phi>1$. It is likely that the flow on upper surface of end plate might be effectively controlled with longer chord length.

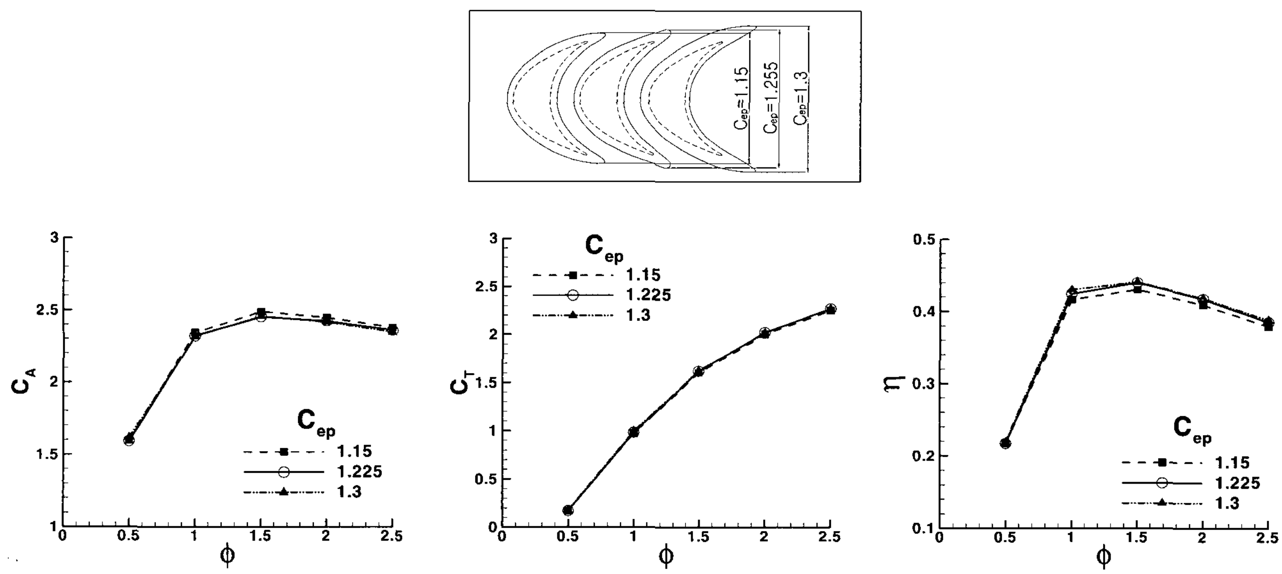

(a) Input Coefficients C_A (b) Torque Coefficients C_T (c) Turbine Efficiency η

Fig. 8 Effect of Chord Length of End Plate

3.4 Effect of Position Bias of End Plate

Figure 9 shows the effect of center location of end plate, the case when the end plate is attached to the rotor blade eccentrically in rotational direction of rotor, where x_{cb} denotes the tangential distance of the center location of end plate biased from that of original blade section. That is, $+x_{cb}$ means the end plate biased toward pressure side, and $-x_{cb}$ biased toward suction side. It should be noted that the present calculation was made with different values of z and G/l_r (z=15 and G/l_r=0.37) to properly accomodate the much larger end plate for clearer demonstration of bias effect.

Standard case (concentric end plate) provides the better performance at ϕ=1, while the case of the end plate biased toward pressure side of rotor blade ($+x_{cb}$) is a little better at ϕ =2.5. End plate biased toward suction side ($-x_{cb}$) yields the worst results for both flow coefficients. The adverse effect in case of $-x_{cb}$ might be inferred from the pattern of flow pathlines on suction side of rotor blade shown in Fig. 10, because the largest vortical flow around trailing edge (TE) region of blade tip could be found for $-x_{cb}$, some evidence of unfavorable flow field creating the higher pressure drop and yielding higher C_A.

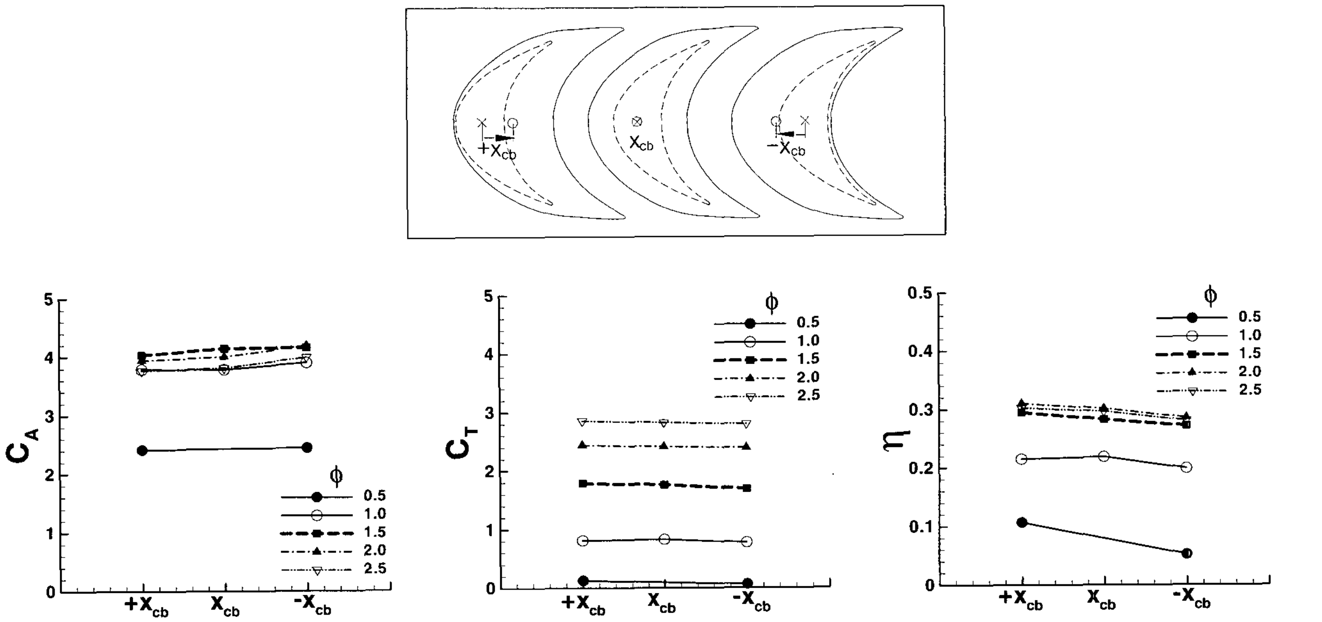

(a) Input Coefficients C_A (b) Torque Coefficients C_T (c) Turbine Efficiency η

Fig. 9 Effect of Position Bias of End Plate

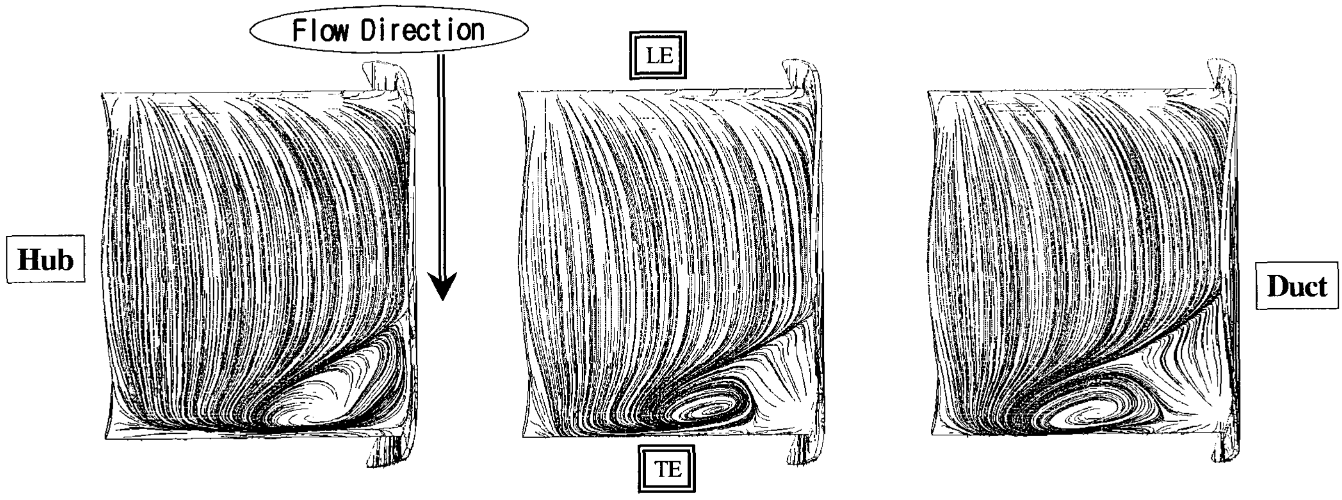

(a) $+x_{cb}$ (b) x_{cb}=0 (c) $-x_{cb}$

Fig. 10 Pathlines on Suction Side of Rotor Blade

4. Summary and Conclusions

This paper deals with the design and analysis of a special-type impulse turbine having an end plate for wave energy conversion. Numerical analysis provided a lot of valuable information and clues to understand the flow physics of impulse turbine well. The present study is summarized as follows;

(1) Grid system was carefully tested to precisely predict the flow field near an end plate. While standard unstructured grid system was adopted, the cooper-type mesh was added to tip region for more grid refinements. Calculated results for original rotor were compared with experiment of Setoguchi et al.(2001) to validate the numerical accuracy.
(2) With an end plate attached to the rotor tip, it was found that the efficiency increases 3~5% depending on flow coefficient for ϕ >1, the higher flow coefficient yielding the better efficiency. The simple penetration of rotor blade, however, doesn't improve the turbine performance at all.
(3) The effects of plate thickness, chord length and eccentricity of an end plate were investigated. While thickness variation of an end plate has a little effect on efficiency, the thinner end plate is better for $\phi < 1$, and the thicker one better for $\phi > 2$. Increase of axial chord length of an end plate tends to improve the efficiency although it is minor. Finally, the concentric end plate gives better results than the eccentric ones, especially an end plate biased toward suction side working very poorly.

Acknowledgments

This research was performed as a part of the project titled "Development of Wave Energy Utilization Technology" supported by Ministry of Marine Affairs and Fisheries (MOMAF), Korea.

References

Hong, S.W. (2004). Development of Wave Energy Utilization Technology, Research Report of KRISO, Unpublished

Hyun, B.-S. and Moon J.-S., (2004). "Analysis of Impulse Turbine for Wave Energy Conversion Using CFD Method", Trans. KCORE, Vol 18, No 5, pp 1~6 (in Korean).

Hyun, B.-S., Moon J.-S., Hong S.W. and Lee Y.Y. (2004). " Practical Numerical Analysis of Impulse Turbine for OWC-type Wave Energy Conversion Using a Commercial CFD Code", Proc. 14th ISOPE, Toulon, France, Vol 1, pp 253~259.

Setoguchi, T., Kinoue Y., Mohammad M., Kaneko K. and Takao M.(2004). "Unsteady Flow Phenomena of Wells Turbine in Deep Stall Condition", Proc. 14th ISOPE, Toulon, France, Vol 1, pp 266~271.

Setoguchi, T., Santhakumar, S. Maeda, H., . Takao, M and K Kaneko (2001). "A Review of Impulse Turbines for Wave Energy Conversion", Renewable Energy, Vol 23, pp 261-292.

2005년 8월 16일 원고 접수
2005년 12월 14일 최종 수정본 채택